Cell Reports Medicine, Volume *4*

Supplemental information

Tumor biology and immune infiltration define primary liver cancer subsets linked to overall survival after immunotherapy

Anuradha Budhu, Erica C. Pehrsson, Aiwu He, Lipika Goyal, Robin Kate Kelley, Hien Dang, Changqing Xie, Cecilia Monge, Mayank Tandon, Lichun Ma, Mahler Revsine, Laura Kuhlman, Karen Zhang, Islam Baiev, Ryan Lamm, Keyur Patel, David E. Kleiner, Stephen M. Hewitt, Bao Tran, Jyoti Shetty, Xiaolin Wu, Yongmei Zhao, Tsai-Wei Shen, Sulbha Choudhari, Yuliya Kriga, Kris Ylaya, Andrew C. Warner, Elijah F. Edmondson, Marshonna Forgues, Tim F. Greten, and Xin Wei Wang

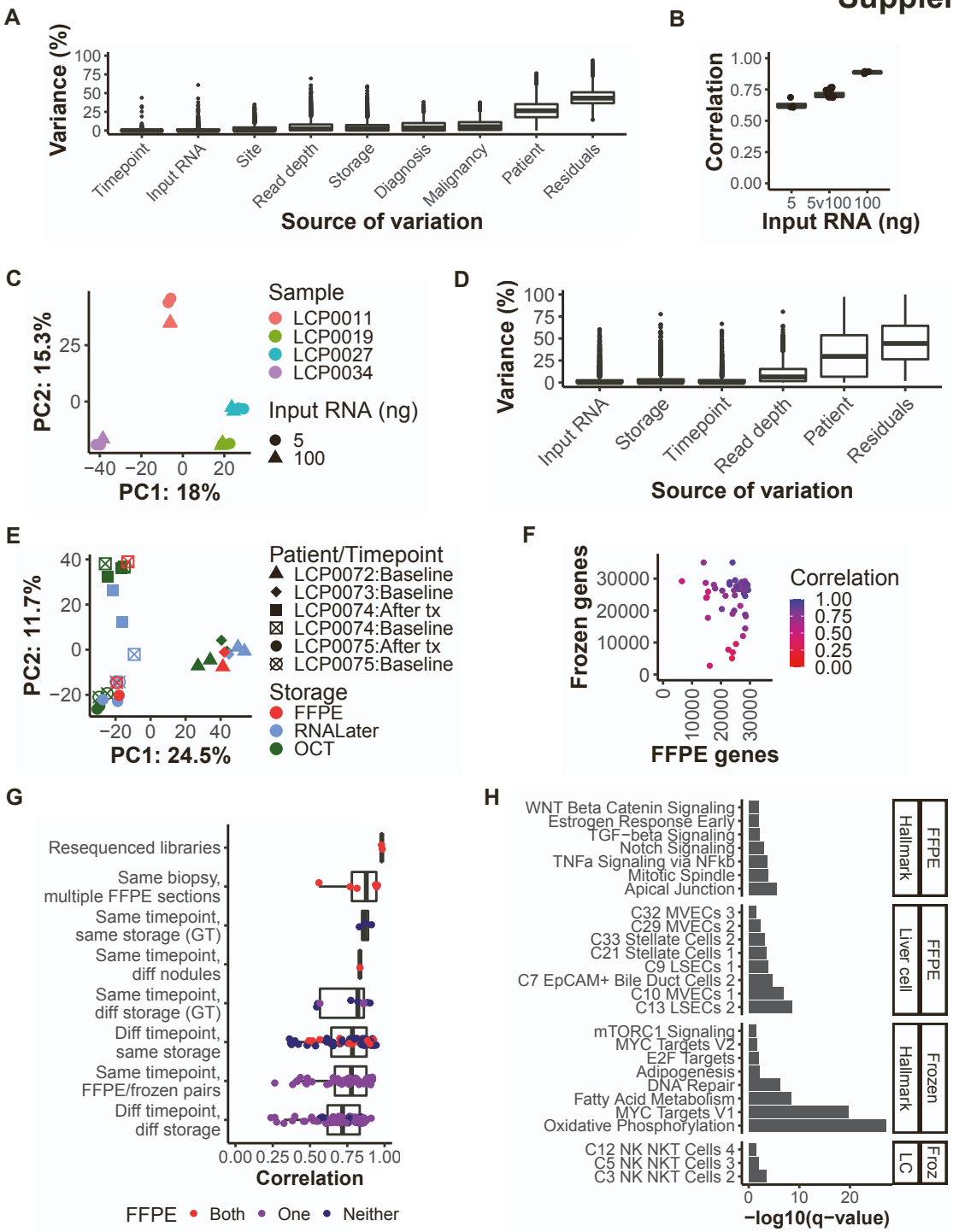

Figure S1. Biological variation outweighs technical variation despite inclusion of archival tissue, Related to STAR Methods. A) Amount of variation in gene expression explained by each variable across all primary liver samples (n=201 samples) for genes with MAD > 2 (n=4,002 genes), as estimated by variancePartition. Each point represents a single gene. Variables are ordered by median. Timepoint: before or after immunotherapy treatment; Input RNA: amount of RNA used to create library (ng); Site: study site; Deduplicated reads: number of deduplicated RNA-seq reads (log10); Storage: method used to store sample (e.g., FFPE, RNALater, OCT block, frozen); Diagnosis: BTC or HCC; Malignancy: tumor or non-tumor; Patient: patient of origin. B) Four liver transplant samples, libraries prepared from 5ng or 100ng of input RNA with two replicates each (n=16 libraries). Pearson correlation between replicates by input RNA amount, ordered by median, top 4,000 most variable genes (by MAD) only (5ng n=4, 5ng vs. 100ng n=16, 100ng n=4 comparisons). C) Principal component analysis (PCA) on the samples from B), using the top 4,000 most variable genes as features (n=16 libraries). D) Six samples from four primary liver cancer patients, each of which was split into three storage methods (n=27 samples passing QC). PCA on the samples using genes with MAD > 2 (n=3,896 genes) as features. E) Amount of variation in gene expression explained by each variable for the samples in Figure S1d (n=27 samples, 3,896 genes), as estimated by variancePartition. Variables are ordered by median. Variable explanations are the same as in Figure S1a. F) Pearson correlation between tumors from the same patient by sample relationship, ordered by median correlation. Correlation is calculated on genes with MAD > 2 across all primary samples. Comparisons are colored by the number of FFPE samples in the sample pair. Resequenced libraries, n=2; multiple FFPE sections, n=6; same storage (GT), n=3; different nodules, n=1; different storage (GT), n=9; different timepoint, same storage, n=67; FFPE/frozen pair, n=49; different timepoint, different storage, n=72. G) Number of genes with any mapped reads in FFPE/frozen sample pairs (n=49 pairs), colored by Pearson correlation across the most variable genes (n=4,002 genes). H) Pathways enriched among DEGs between FFPE/frozen sample pairs, ordered by FDR-corrected p-value (n=9,725 genes with adjusted p-value < 0.05). Genes were split by whether they were more highly expressed in FFPE or frozen samples, and enriched gene sets are divided into MSigDB Hallmark and c8 liver cell types. (A, B, D and G) Boxplots: center line, median; box limits, first and third quartiles; whiskers, values ≤1.5 times the interquartile range from box limits; points, outliers.

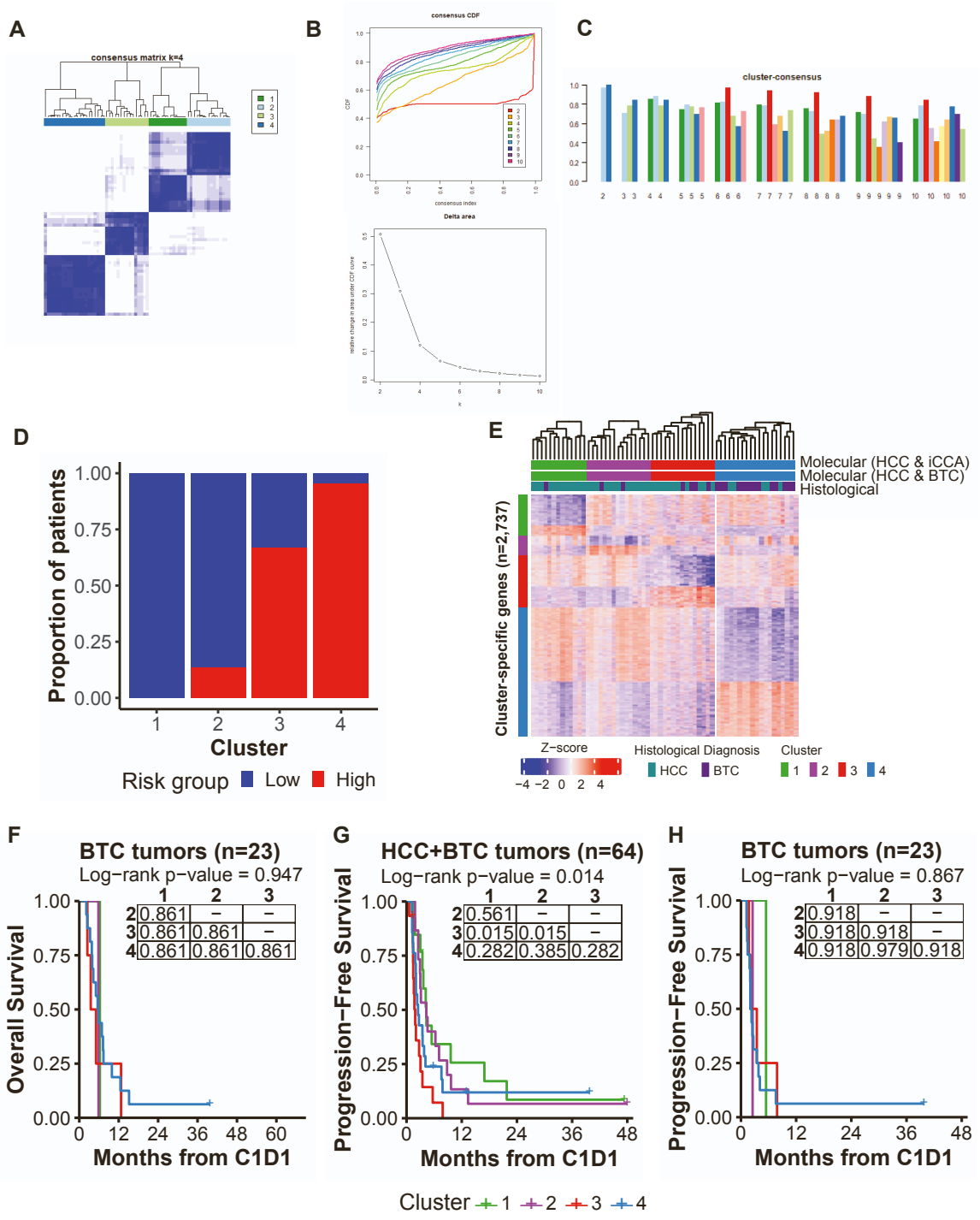

Figure S2. Consensus clustering of baseline tumors and survival differences, Related to Figure 2. A) Consensus index heatmap for baseline tumors (n=64 tumors) using the k=4 solution, i.e., the proportion of iterations in which two samples clustered together out of all iterations in which both samples were selected. Mean cluster consensus score within clusters was 0.84. B) Upper panel: Cumulative density functions (CDF) for the consensus index across all sample pairs, k=2-10 solutions. A greater proportion of indices at 0 or 1 indicates cleaner clustering. Lower panel: Delta area under the curve for the cumulative density functions in B), k=2-10 solutions. C) Mean consensus index values for samples assigned to each cluster, k=2-10 solutions. D) Proportion of baseline tumors in each molecular cluster assigned to each survival risk group (cluster 1, n=13 tumors; cluster 2, n=15; cluster 3, n=15; cluster 4, n=21). E) Semi-supervised hierarchical clustering of baseline tumors on cluster-specific differentially expressed genes. Tumors were clustered using Euclidean distance with complete linkage within each cluster and are labelled with the cluster assignments generated using all cases (Molecular HCC & BTC) or excluding extrahepatic CCA (Molecular HCC & iCCA). Heatmap displays expression Z-scores by row. F) Kaplan-Meier curve for overall survival probability since C1D1 of immunotherapy by molecular cluster, BTC tumors only (cluster 1, n=1 tumor; cluster 2, n=2; cluster 3, n=4; cluster 4, n=16). G) Kaplan-Meier curve for progression-free survival probability since C1D1 of immunotherapy by molecular cluster, all baseline tumors (same n's as in Figure S2e). H) Kaplan-Meier curve for progression-free survival probability since C1D1 of immunotherapy by molecular cluster, BTC tumors (same n's as in Figure S2f). F-H) The overall log-rank test p-value is listed above the graph. The embedded table presents pairwise log-rank test p-values with BH correction. Cluster legend is below panels.

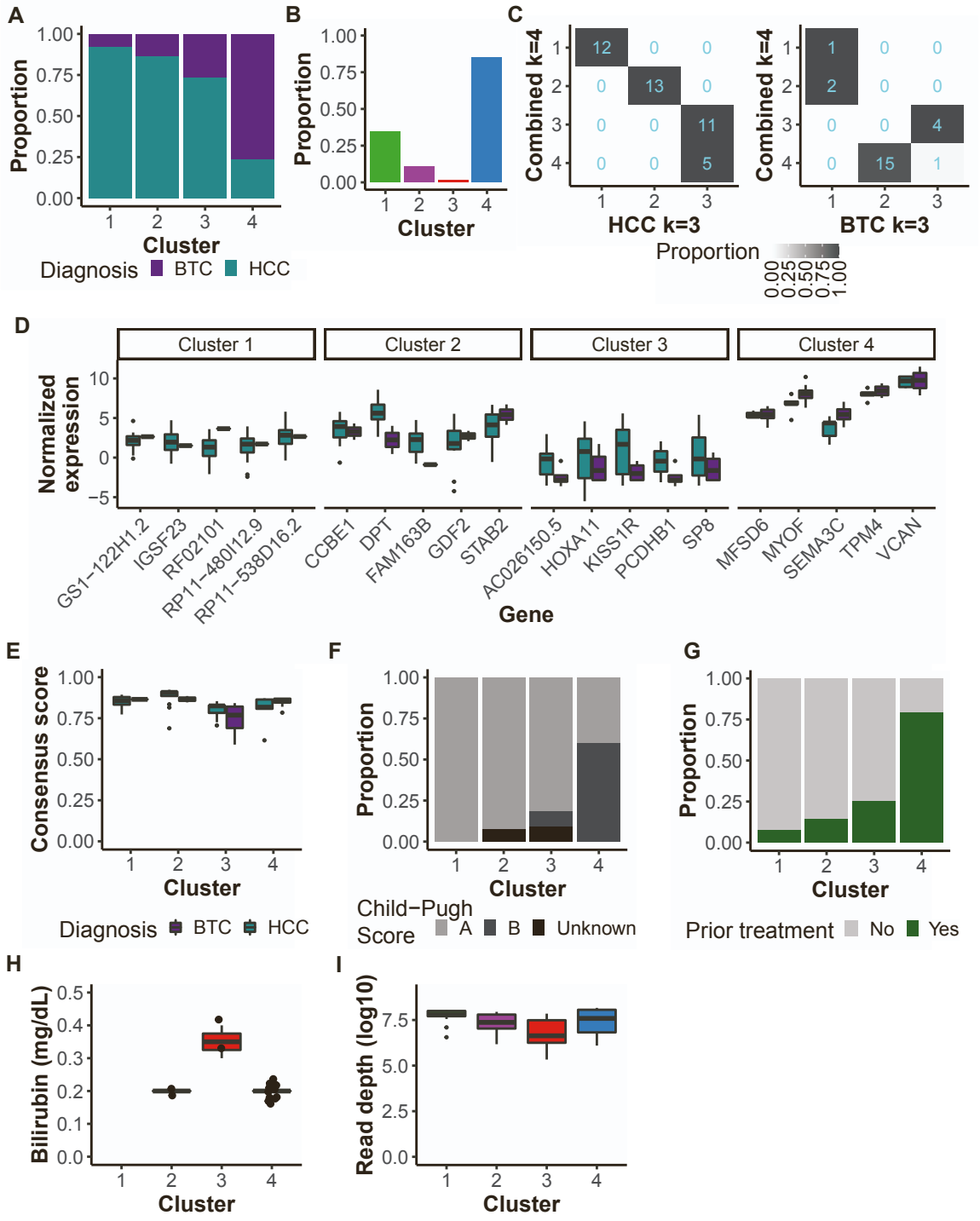

Figure S3. Clinical data associated with baseline tumor clusters, Related to Figure 2. A) Proportion of patients with each histological diagnosis (cluster 1, n=13 tumors; cluster 2, n=15; cluster 3, n=15; cluster 4, n=21). B) Proportion of cluster-specific DEGs that are also DEGs between HCC and BTC baseline tumors (cluster 1, n=490 DEGs; cluster 2, n=237; cluster 3, n=611; cluster 4, n=1,638). C) Proportion of samples in each molecular cluster (y-axis) assigned to each independently generated HCC or BTC cluster (x-axis). Tiles are labelled with the number of samples. D) For each molecular cluster, the top 5 upregulated DEGs (ranked by lowest maximum p-value versus each other cluster). Boxplots include samples in that cluster, split by diagnosis (HCC: cluster 1, n=12 tumors; cluster 2, n=13; cluster 3, n=11; cluster 4, n=5; BTC: cluster 1, n=1 tumor; cluster 2, n=2; cluster 3, n=4; cluster 4, n=16). See Figure S3a for diagnosis legend. E) Item consensus score for each sample for its assigned molecular cluster, split by diagnosis (same n's as Figure S3d). F) Proportion of HCC patients with each Child-Pugh score at baseline (cluster 1, n=12 tumors; cluster 2, n=13; cluster 3, n=11; cluster 4, n=5). G) Proportion of patients with prior treatment with systemic multiagent chemotherapy (patients with known prior treatment status only; Chi-squared test, FDR-adjusted p-value = 0.001; cluster 1, n=13 tumors; cluster 2, n=14; cluster 3, n=12; cluster 4, n=19). H) Direct bilirubin level at baseline (BTC only, cluster 1, n=0 tumors; cluster 2, n=2; cluster 3, n=2; cluster 4, n=14; Kruskal-Wallis test p-value = 0.007). I) De-duplicated RNA-seq read depth of baseline tumor samples (Kruskal-Wallis test, p-value = 0.02; same n's as in Figure S3a). (D, E, H and I) Boxplots: center line, median; box limits, first and third quartiles; whiskers, values ≤1.5 times the interquartile range from box limits; points, outliers.

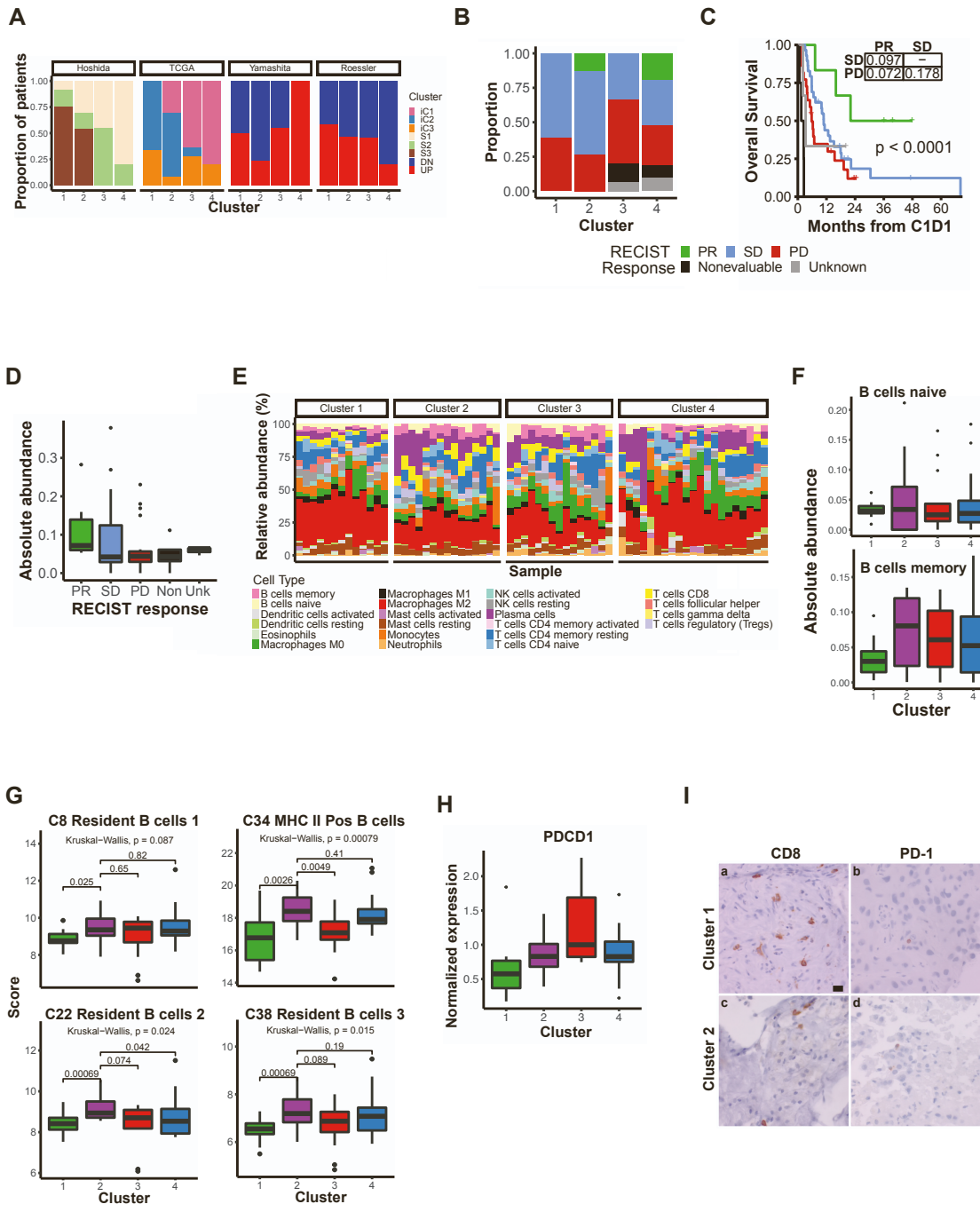

Figure S4. Previous subclasses, RECIST response, and immune profiling of baseline tumors, Related to Figure 2. A) Subclass assignments by molecular cluster for HCC baseline tumors, using signatures developed in18-20,53. Cluster 1, n=12 tumors; cluster 2, n=13; cluster 3, n=11; cluster 4, n=5. B) Proportion of patients with best RECIST response (RECIST v1.1) on immunotherapy by molecular cluster (cluster 1, n=13 tumors; cluster 2, n=15; cluster 3, n=15; cluster 4, n=21). Legend below Figure S4C. C) Kaplan-Meier curve for overall survival probability since C1D1 of immunotherapy by RECIST response, all baseline tumors (PR, n=6 tumors; SD, n=29; PD, n=22; Non-evaluable, n=4; Unknown, n=3). The overall log-rank test p-value is listed above the graph. The embedded table presents pairwise log-rank test p-values between PR, SD, and PD patients with BH correction. D) CIBERSORTx LM22 cell types enriched in responders vs. non-responders (Wilcox test, uncorrected p-value < 0.05; n's as in Figure S4c). Non: Non-evaluable; Unk: Unknown. E) Relative abundance of each LM22 cell type in baseline tumors, as estimated by CIBERSORTx. Samples are ordered based on hierarchical clustering on cell type relative abundances (1-Pearson correlation, complete linkage). Cluster 1, n=13 tumors; cluster 2, n=15; cluster 3, n=15; cluster 4, n=21. F) CIBERSORTx LM22 naïve and memory B cells (cluster 1, n=13 tumors; cluster 2, n=15; cluster 3, n=15; cluster 4, n=21). G) MSigDB Hallmark B cell gene sets. Pairwise comparisons between cluster 2 and each other cluster are shown (Wilcox test) as well as a global p-value (Kruskal-Wallis test). H) Immune checkpoint expression by molecular cluster normalized by CD3 expression (same n's as in Figure 4e). I) Immunohistochemistry for CD8 (a&c) and PD-1 (b&d) from representative samples from C1 (a&b) and C2 (c&d). Both CD8 samples were scored 2 (scattered) and both PD-1 samples are scored 1 (rare). 400X magnification, scale bar equals 10 um. (D, F, G and H) Boxplots: center line, median; box limits, first and third quartiles; whiskers, values ≤1.5 times the interquartile range from box limits; points, outliers.

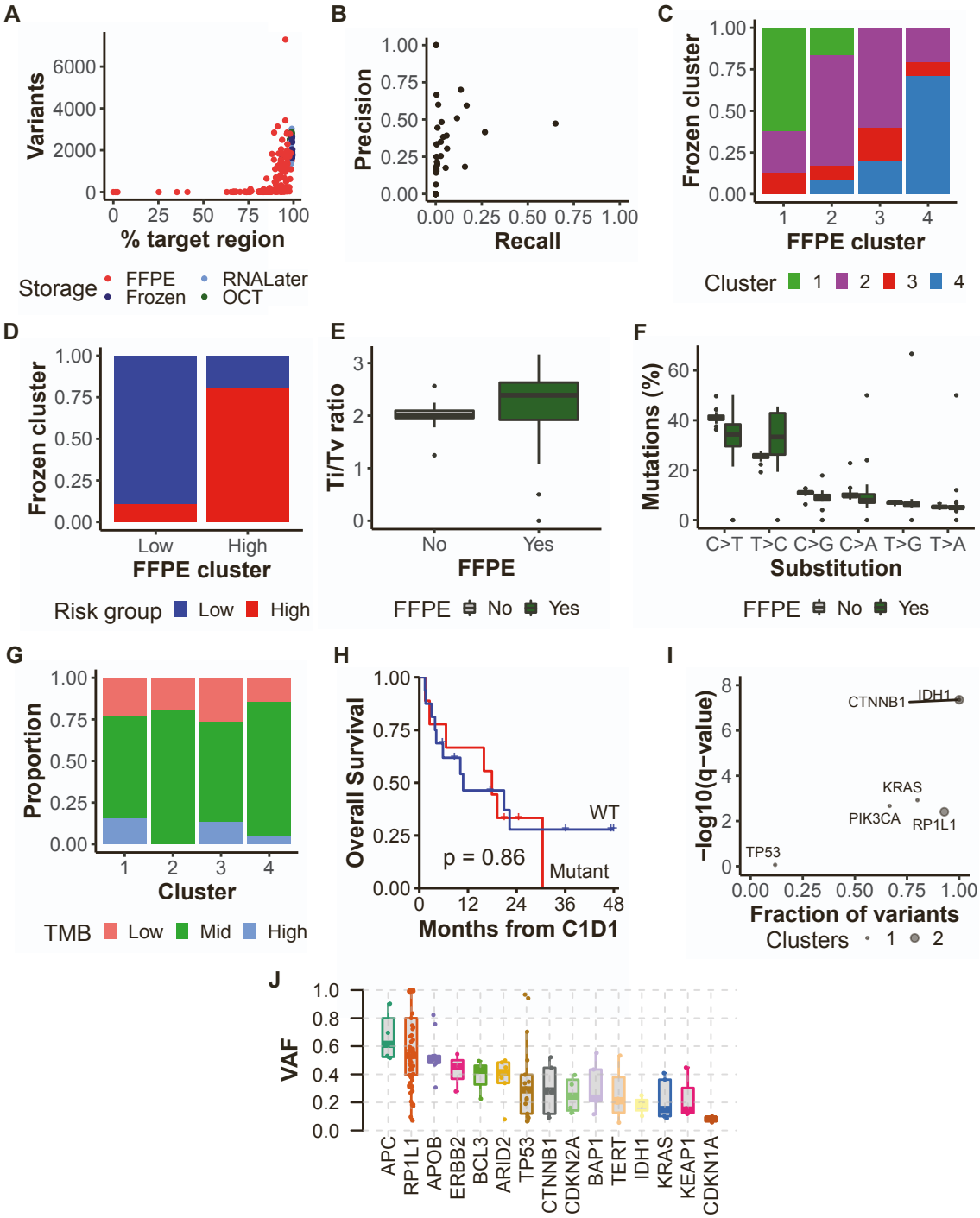

Figure S5. Concordance of FFPE/frozen sample pairs and known driver mutations in baseline tumors, Related to Figure 5. A) Percent of target region with coverage > 20X vs. number of somatic variants, colored by storage method (n=226 primary liver samples from immunotherapy patients). B) Precision (TP/(TP+FP)) and recall (TP/(TP+FN)) for non-silent somatic variants identified in FFPE/frozen sample pairs, using the frozen sample as truth (54 pairs, 9 excluded from plot due to no FFPE variant). C) Cluster assignments for FFPE/frozen sample pairs (n=49 pairs). The y-axis represents the proportion of frozen samples. If available, the cluster assigned by consensus clustering was used. D) Survival risk group assignments for FFPE/-frozen sample pairs (n=49 pairs). The y-axis represents the proportion of frozen samples. E) Transition/Transversion (Ti/Tv) ratio for baseline tumor SNVs by storage method, including synonymous mutations (FFPE n=21 tumors, non-FFPE n=42). F) Substitution category for baseline tumor SNVs by storage method, including synonymous mutations, ordered by median (FFPE n=21 tumors, non-FFPE n=42). G) Proportion of baseline tumors assigned to each molecular cluster by TMB level (Low, <10 variants/Mb; Mid, 10-20 variants/Mb; High, >20 variants/Mb, based on distributions across samples in this study; cluster 1, n=13 tumors; cluster 2, n=15; cluster 3, n=15; cluster 4, n=21). H) Kaplan-Meier curve of overall survival probability by TP53 mutation status among non-FFPE HCC baseline tumors (WT n = 16 tumors, mutated n = 9). Only non-silent variants were considered. The log-rank test p-value is presented. CLIN_SIG status of TP53 mutations: 6/9 “pathogenic” or “likely_pathogenic”, 1/9 “uncertain_significance”, 2/9 no entry. I) Hotspot analysis of known driver genes in baseline tumors using the OncodriveCLUST algorithm implemented by maftools. A gene required at least one mutation to be included in the analysis. The fraction of variants in clusters (x-axis) vs. the FDR-corrected p-value (y-axis) is shown. J) Variant allele frequency (VAF) distribution among baseline tumors for mutations in known driver genes (top 15). Genes are ordered by decreasing median. (E, F and J) Boxplots: center line, median; box limits, first and third quartiles; whiskers, values ≤1.5 times the interquartile range from box limits; points, outliers.

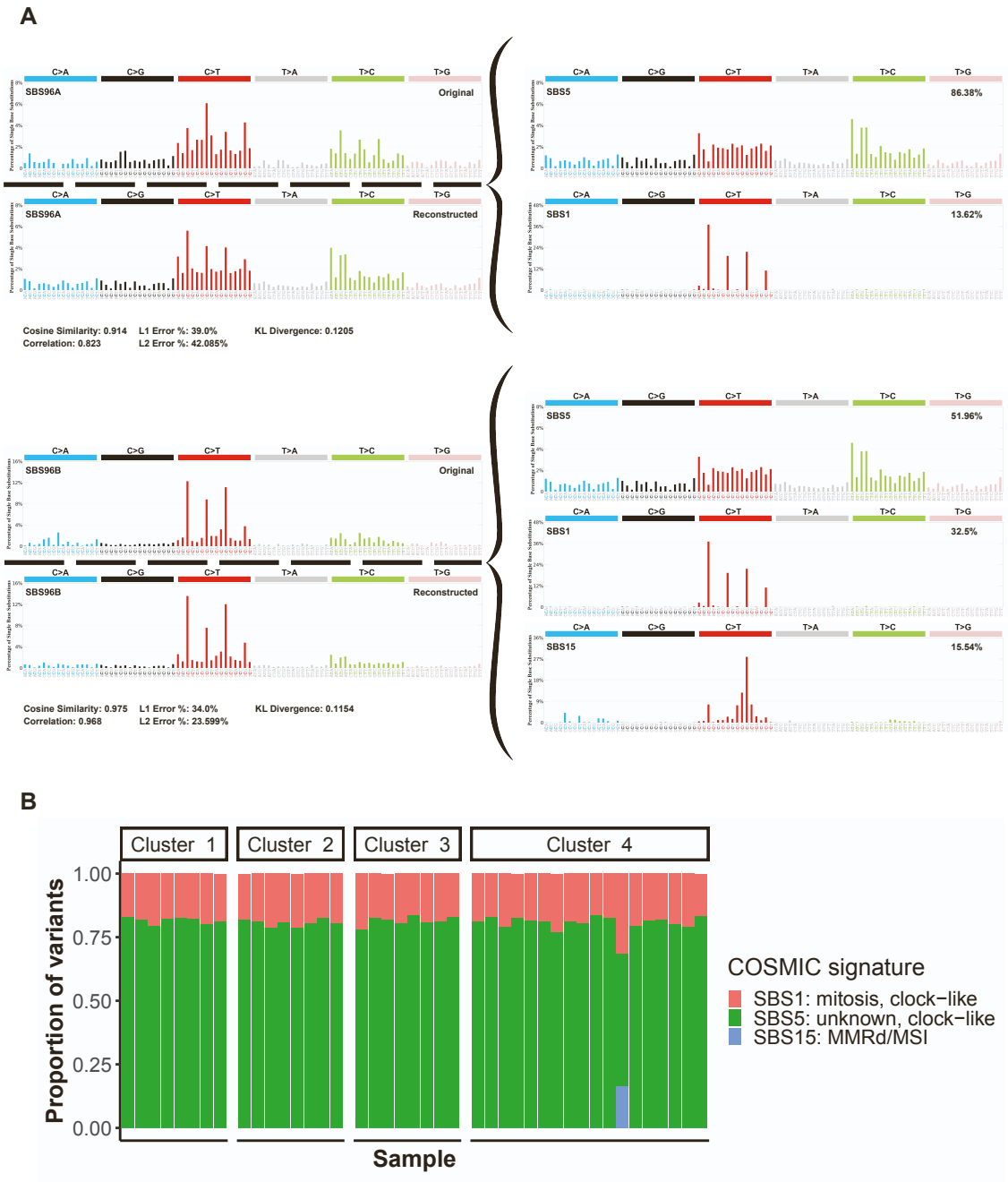

Figure S6. Mutation signatures in baseline tumors, Related to Figure 5. A) Estimated contribution of COSMIC signatures to each non-FFPE baseline tumor by molecular cluster (cluster 1, n=8 tumors; cluster 2, n=8 tumors; cluster 3, n=8 tumors; cluster 4, n=18 tumors). B) Decomposition of two de novo signatures into COSMIC signatures. For each signature, the original and reconstructed signatures are presented, as well as the constituent COSMIC signatures.

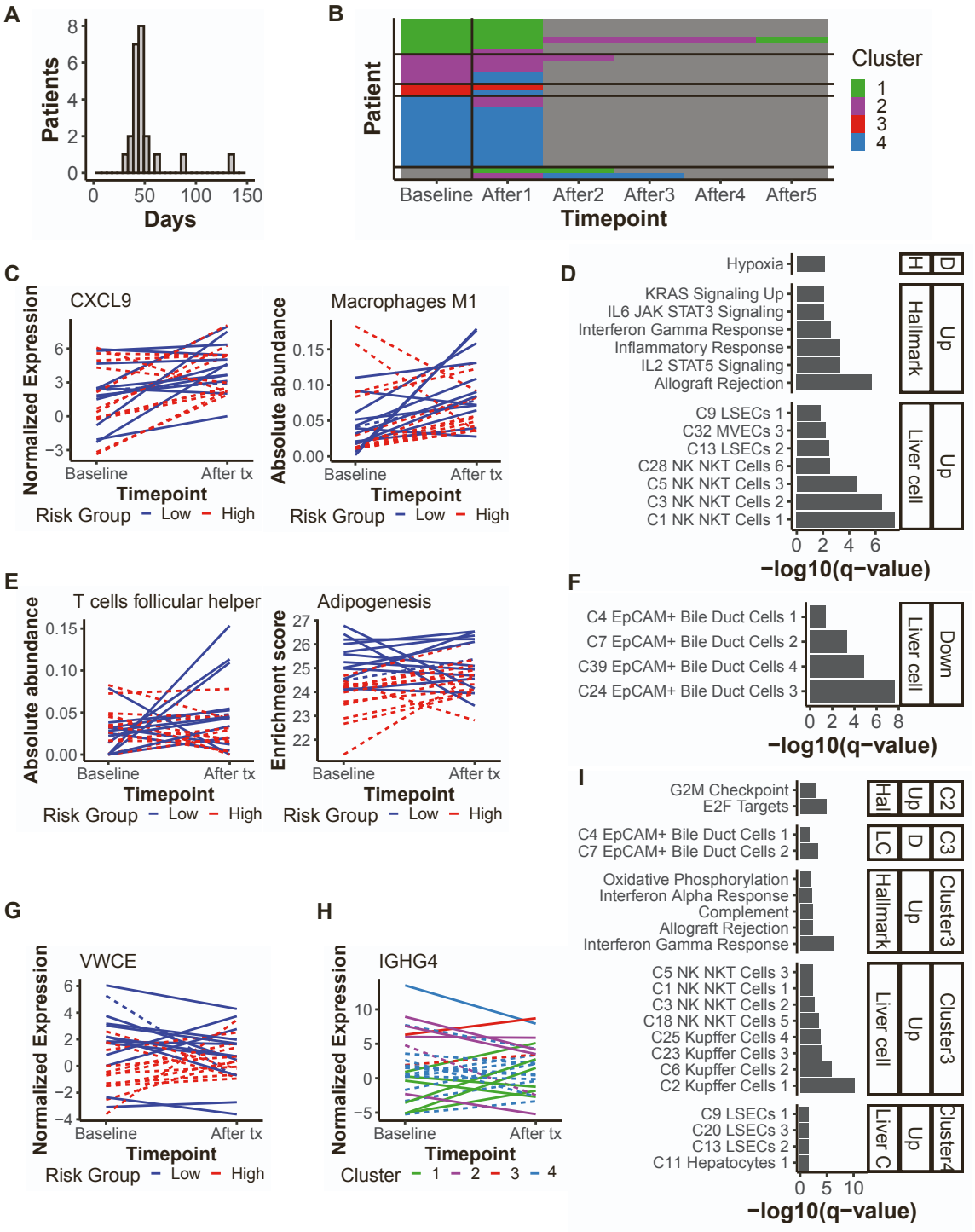

Figure S7. After-treatment tumors, Related to Figure 7. A) Days between baseline and after-treatment tumor collection for 23 sample pairs with available dates. B) Cluster assignments for patients with paired baseline and after-treatment tumors and/or treatment timecourses (n=27 patients). C) Left panel: Normalized gene expression over time in paired tumors for CXCL9. Right panel: Absolute abundance over time in paired tumors for the CIBERSORTx cell type Macrophages M1. D) Pathways enriched among DEGs between baseline and after-treatment tumors (n=243 genes, uncorrected p-value < 0.01). E) Left panel: Absolute abundance over time in paired tumors for the CIBERSORTx cell type T cells follicular helper. Right panel: Enrichment score over time in paired tumors for the MSigDB Hallmark adipogenesis gene set. F) Pathways enriched among DEGs with interactions with survival risk group (n=122 genes, uncorrected p-value < 0.01). G) Normalized gene expression over time in paired tumors for VWCE. H) Normalized gene expression over time in paired tumors for IGHG4. I) Pathways enriched among DEGs with interactions with molecular cluster (Cluster 2, n=110 genes; Cluster 3, n=895; Cluster 4, n=75; uncorrected p-value < 0.01). C, E, G, H) Lines are colored by the predicted risk group or molecular cluster of the baseline tumor. Dashed lines represent BTC; solid lines represent HCC. n=25 pairs. D, F, I) Genes were split by whether they were relatively up- or downregulated after treatment initiation (overall, in the high-risk survival group, or in each cluster vs. cluster 1), and gene sets are divided into MSigDB Hallmark (H) and c8 liver cell (LC) types. Gene sets are ordered by FDR-corrected p-value.

Supplemental information table titles

Table S1. Survival signature genes, Related to Figure 1

Table S2. Molecular cluster-specific DEGs, Related to Figure 2.

Table S3. Clinical data tested for association with molecular clusters, Related to Figure 2.

Table S4. Prior treatment data tested for association with molecular clusters, Related to Figure 2.

Table S5. DEGs between responders and non-responders at baseline, Related to Figure 3.

Table S6. DEGs between tumors before and following treatment, Related to Figure 6.

Supplementary Table 3. Clinical data tested for association with molecular clusters. Related to Figure 2.

		All baseline tumors			HCC baseline tumors			BTC baseline tumors		
Variable	**Test**	**n***	**p-value**	**adjusted p-value**	**n***	**p-value**	**adjusted p-value**	**n***	**p-value**	**adjusted p-value**
Study site	Chi-squared	64	0.296	0.534	41	0.882	0.918	23	0.163	0.955
Diagnosis	Chi-squared	64	0.000	0.004						
Race	Chi-squared	62	0.037	0.239	39	0.608	0.918	23	0.305	0.955
Ethnicity	Chi-squared	63	0.083	0.248	41	0.095	0.333	22	0.318	0.955
Gender	Chi-squared	64	0.320	0.534	41	0.176	0.397	23	0.700	1.000
BMI	Kruskal-Wallis	64	0.507	0.630	41	0.814	0.918	23	0.364	1.000
ECOG	Chi-squared	55	0.054	0.245	36	0.019	0.169	19	0.663	1.000
Age at Diagnosis	Kruskal-Wallis	58	0.626	0.718	38	0.737	0.918	20	0.636	1.000
Prior Surgery	Chi-squared	57	0.948	0.948	37	0.615	0.918	20	0.878	1.000
Prior Treatment	Chi-squared	58	0.328	0.534	37	0.858	0.918	21	0.279	0.955
HBV STATUS	Chi-squared	64	0.056	0.245	41	0.164	0.397	23	0.541	1.000
HCV STATUS	Chi-squared	64	0.297	0.534	41	0.732	0.918	23	1.000	1.000
HCV Treated	Chi-squared	51	0.789	0.831	33	0.864	0.918	18	1.000	1.000
Cirrhosis	Chi-squared	64	0.353	0.551	41	0.167	0.397	23	0.526	1.000
Diabetes	Chi-squared	64	0.277	0.534	41	0.349	0.673	23	0.414	1.000
EtOH Abuse	Chi-squared	64	0.424	0.570	41	0.071	0.331	23	1.000	1.000
Haemachromatosis	Chi-squared	63	0.662	0.731				23	0.305	0.955
Steatohepatitis (NASH, Fatty Liver)	Chi-squared	59	0.517	0.630	36	0.877	0.918	23	0.520	1.000
AFP (ng/mL)	Kruskal-Wallis	59	0.068	0.248	40	0.083	0.331	19	0.796	1.000
ALT (u/L)	Kruskal-Wallis	53	0.573	0.677	34	0.741	0.918	19	0.293	0.955
AST (u/L)	Kruskal-Wallis	53	0.175	0.426	34	0.140	0.397	19	0.831	1.000
BILIRUB_DIR (mg/dl)	Kruskal-Wallis	44	0.030	0.239	26	0.467	0.800	18	0.000	0.008
BILIRUB_TTL (mg/dl)	Kruskal-Wallis	58	0.017	0.216	38	0.076	0.331	20	0.119	0.955
Ca 19-9 (U/mL)	Kruskal-Wallis	42	0.329	0.534	21	0.355	0.673	21	0.906	1.000
Child Score	Chi-squared	59	0.246	0.534	39	0.001	0.047	20	0.119	0.955
BCLC Stage	Chi-squared	62	0.410	0.570	41	0.638	0.918	21	1.000	1.000
Extraheptic Spread	Chi-squared	57	0.082	0.248	37	0.562	0.918	20	0.784	1.000
Microvascular Invasion	Chi-squared	21	0.004	0.070	18	0.008	0.124	3	1.000	1.000
Tumor Encapsulation	Chi-squared	15	0.402	0.570						
Differentiation Status Descriptor	Chi-squared	41	0.032	0.239	21	0.010	0.124	20	0.496	1.000
Multinodular	Chi-squared	61	0.447	0.582	39	0.829	0.918	22	0.087	0.955
Main Tumor Size	Kruskal-Wallis	64	0.076	0.248	41	0.176	0.397	23	0.149	0.955
Treatment category	Chi-squared	64	0.675	0.731	41	0.913	0.918	23	0.447	1.000
ICI Target	Chi-squared	64	0.055	0.245	41	0.436	0.785	23	0.217	0.955
Best of Response	Chi-squared	61	0.214	0.490	40	0.049	0.297	21	0.788	1.000
Time to Best Response	Kruskal-Wallis	15	0.166	0.426	14	0.260	0.550			
Responder	Chi-squared	57	0.105	0.293	37	0.028	0.204	20	1.000	1.000
Radiation Treatment	Chi-squared	43	0.393	0.570	23	0.102	0.333	20	0.573	1.000
Follow-up Treatment	Chi-squared	22	0.838	0.860	19	0.918	0.918	3	1.000	1.000

*n indicates total number of patients tested

Supplementary Table 4. Prior treatment data tested for association with molecular clusters. Related to Figure 2.

	All baseline tumors			HCC baseline tumors			BTC baseline tumors		
Prior Treatment	**n***	**p-value**	**adjusted p-value**	**n***	**p-value**	**adjusted p-value**	**n***	**p-value**	**adjusted p-value**
Antisense	1	0.675	0.921	1	1.000	1.000			
Chemoembolization	16	0.021	0.103	16	0.586	1.000			
Chemotherapy Multiple Agent Systemic	21	0.000	0.001	1	0.356	1.000	20	0.296	0.889
Chemotherapy Non-Cytotoxic	13	0.742	0.921	9	0.944	1.000	4	0.546	0.964
Chemotherapy Single Agent Systemic	6	0.829	0.921	1	1.000	1.000	5	0.803	0.964
Drug and/or Immunotherapy	2	0.138	0.230	2	0.452	1.000			
Prior Therapy (NOS)	4	0.092	0.185	4	0.266	1.000			
Radiation (NOS)	9	1.000	1.000	4	0.709	1.000	5	0.182	0.889
Radioembolization	10	0.043	0.144	7	0.051	0.508	3	1.000	1.000
Surgery	9	0.082	0.185	2	0.781	1.000	7	0.719	0.964

*n indicates number of patients with prior treatment among those with known treatment status (n=58)